Clin Orthop Relat Res (2014) 472:665–673
DOI 10.1007/s11999-013-3127-z

Clinical Orthopaedics and Related Research®
A Publication of The Association of Bone and Joint Surgeons®

SYMPOSIUM: 2013 HIP SOCIETY PROCEEDINGS

Hip Dysplasia Is More Severe in Charcot-Marie-Tooth Disease Than in Developmental Dysplasia of the Hip

Eduardo N. Novais MD, Sara D. Bixby MD, John Rennick MSc, Patrick M. Carry BA, Young-Jo Kim MD, PhD, Michael B. Millis MD

Published online: 14 August 2013

Abstract

Background Patients with Charcot-Marie-Tooth disease may develop hip dysplasia. Hip geometry in these patients has not been well described in the literature.

Questions/purposes We compared the hip morphometry in Charcot-Marie-Tooth hip dysplasia (CMTHD) and developmental dysplasia of the hip (DDH) in terms of extent of (1) acetabular dysplasia and subluxation, (2) acetabular anteversion and osseous support, (3) coxa valga and femoral version, and (4) osteoarthritis.

Methods Fourteen patients with CMTHD (19 hips; mean age, 23 years) presenting for periacetabular osteotomy were matched to 45 patients with DDH (45 hips; mean age, 21 years) based on age, sex, and BMI. We assessed acetabular dysplasia and subluxation using lateral center-edge angle (LCEA), anterior center-edge angle (ACEA), and acetabular roof angle of Tönnis (TA) on plain pelvic radiographs and acetabular volume, area of femoral head covered by acetabulum, and percentage of femoral head covered by acetabulum on three-dimensional CT reconstruction models. Acetabular version and bony support, femoral version, and neck-shaft angle were measured on two-dimensional axial CT scans. Hip osteoarthritis was graded radiographically according to Tönnis criteria.

Results Acetabular dysplasia was more severe in CMTHD, as measured by smaller LCEA ($p < 0.001$), ACEA ($p < 0.001$), and acetabular volume ($p = 0.0178$) and larger TA ($p = 0.025$). Hip subluxation was more pronounced in CMTHD, as demonstrated by lower area of femoral head covered by acetabulum ($p = 0.034$) and percentage of femoral head covered by acetabulum ($p = 0.007$). CMTHD was associated with higher acetabular anteversion ($p < 0.001$), lower anterior ($p < 0.001$) and posterior ($p = 0.072$) osseous support, and more severe coxa valga ($p < 0.001$). More ($p = 0.006$) arthritic hips were found in CMTHD.

Each author certifies that he or she, or a member of his or her immediate family, has no commercial associations (eg, consultancies, stock ownership, equity interest, patent/licensing arrangements, etc) that might pose a conflict of interest in connection with the submitted article.
All ICMJE Conflict of Interest Forms for authors and *Clinical Orthopaedics and Related Research* editors and board members are on file with the publication and can be viewed on request.
Each author certifies that his or her institution approved the human protocol for this investigation, that all investigations were conducted in conformity with ethical principles of research, and that informed consent for participation in the study was obtained.
This work was performed at Boston Children's Hospital, Boston, MA, USA.

E. N. Novais, P. M. Carry
Department of Orthopedic Surgery, Children's Hospital Colorado, University of Colorado School of Medicine, Aurora, CO, USA

S. D. Bixby
Department of Radiology, Boston Children's Hospital, Boston, MA, USA

J. Rennick
Northeastern University, Boston, MA, USA

Y.-J. Kim, M. B. Millis (✉)
Department of Orthopedic Surgery, Boston Children's Hospital, 300 Longwood Avenue, Hunnewell 213, Boston, MA 02115-5724, USA
e-mail: Michael.millis@childrens.harvard.edu; michael.millis@tch.harvard.edu

Conclusions The extent of acetabular dysplasia, hip subluxation, acetabular anteversion, coxa valga, and hip osteoarthritis was more severe in CMTHD. These findings are important in choosing the appropriate surgical strategy for patients affected by CMTHD.
Level of Evidence Level IV, diagnostic study. See Instructions for Authors for a complete description of levels of evidence.

Introduction

Charcot-Marie-Tooth disease (CMT) affects approximately 36 in 10,000 people [15]. CMT represents a heritable peripheral neuropathy that is associated with progressive motor disability and sensory loss [5, 7]. In addition to distal lower-extremity weakness, hip abductor and/or hip extensor weakness is present in a subgroup of patients affected by CMT [7, 16, 17, 27]. This proximal hip weakness has been suggested to create a muscular imbalance about the hip that may result in acetabular dysplasia, increased femoral neck-shaft angle (NSA) (coxa valga), and femoral anteversion [7].

The prevalence of hip dysplasia among patients with CMT is estimated to be 6% to 8.1% [42]. The association between hip dysplasia and CMT was first described by Kumar et al. [16]. The literature on CMT hip dysplasia (CMTHD) is limited to isolated case series reports, and there is limited information regarding the pathophysiology, hip geometry, and natural history of CMTHD [5, 7, 16, 22, 29, 40, 42]. The age at presentation and severity of hip dysplasia vary widely due to the heterogeneous clinical expression of the disorder [7, 42, 46]. Even in cases of severe dysplasia, the presence of pain has been reported to be a later manifestation of CMTHD [16, 40, 42]. Operative treatment is generally recommended for addressing CMTHD [7, 16, 41, 46]. Several corrective pelvic osteotomies, including the Chiari osteotomy [42], triple osteotomy [41], Bernese periacetabular osteotomy (PAO) [36, 39], and Salter innominate osteotomy [16, 22], have been described. However, surgical correction of CMTHD is challenging and a high risk of complications, including injury of the sciatic nerve, has been previously reported [16].

Numerous studies have characterized the abnormal hip morphology secondary to developmental dysplasia of the hip (DDH) [6, 12, 14, 20, 24, 30, 34, 44]. However, the geometry of the dysplastic hip secondary to CMT has not been well described in current literature. Surgical correction of CMTHD should consider the complex three-dimensional (3-D) deformity of the acetabulum and proximal femur. We therefore determined whether there was a difference in the morphology of the hip between patients affected by CMTHD and those affected by DDH in terms of (1) severity of acetabular dysplasia and subluxation, (2) acetabular anteversion and osseous support, (3) severity of coxa valga and femoral version, and (3) severity of osteoarthritis at the time of presentation for PAO.

Patients and Methods

We used a retrospective observational study design to compare hip morphology between patients affected by CMTHD and those affected by DDH at the time of presentation for PAO. A query of the orthopaedic surgical database at our institution identified 1080 Bernese PAOs performed for the treatment of hip dysplasia between January 1991 and December 2010. Thirty-five PAOs were performed in 27 patients with documented diagnosis of CMT (confirmed by a neurologist) and associated symptomatic hip dysplasia (diagnosed based on a history of hip pain and radiographs revealing a lateral center-edge angle [LCEA] of Wiberg [45] $< 20°$). Eight patients with previous pelvic or femoral osteotomies and five patients with no CT scans were excluded. Patients with CMTHD were then matched to patients with hip dysplasia secondary to DDH who also had presented for Bernese PAO on the basis of sex, age at surgery ($\pm$ 3 years), date of surgery ($\pm$ 3 years), and BMI ($\pm$ 3 units). For the matching process, patients with hip dysplasia secondary to Legg-Calvé-Perthes disease and/or neuromuscular disorders, as well as patients with no available preoperative CT scan of the pelvis, were excluded. A total of 58 patients with a primary diagnosis of DDH were matched to the CMT cohort. Thirteen patients with a previous history of hip surgery, including open reduction of the hip and pelvic or femoral osteotomies, were further excluded. The study included 14 patients (19 hips) with CMTHD and 45 patients (45 hips) with DDH. With the numbers available, there was no difference in sex ($p = 0.0899$), age ($p = 0.6770$), or BMI ($p = 0.2095$) between groups (Table 1). This study was based on review of medical charts and imaging only, and institutional review board approval was obtained before the review and analysis of all study-related data.

Severity of acetabular dysplasia was assessed on standing AP and false-profile radiographs of the pelvis. A hip preservation surgeon not involved in the clinical care of the patients (ENN) measured the LCEA of Wiberg [45] and the acetabular roof obliquity angle of Tönnis (TA) [37] on the AP radiographs and the anterior center-edge angle (ACEA) of Lequesne and de Séze [18] on the false-profile radiographs. To further evaluate the severity of acetabular dysplasia and the degree of hip subluxation, acetabular volume, acetabular area, femoral head area, area of the femoral head covered by the acetabulum, and percentage of the femoral head covered by the acetabulum were assessed

Table 1. Demographics and clinical characteristics

Variable	CMTHD group (n = 19)	DDH group (n = 45)	p value
Age (years)*	23 ± 8	22 ± 8	0.6770
BMI*	26 ± 8	24 ± 5	0.2095
Sex (number of patients)			0.0899
Female	7 (37%)	27 (60%)	
Male	12 (63%)	18 (40%)	

* Values are expressed as mean ± SD; CMTHD = Charcot-Marie-Tooth hip dysplasia; DDH = developmental dysplasia of the hip.

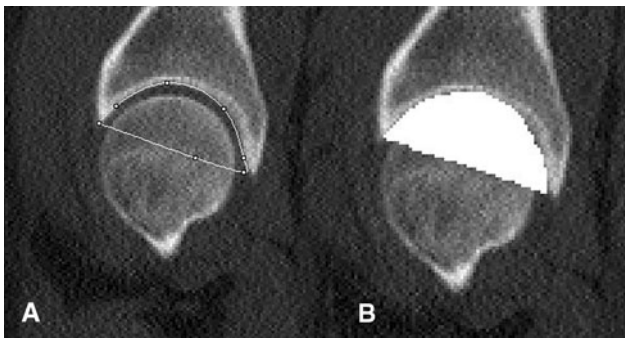

Fig. 1A–B The procedures used to define the volume of the acetabulum in ImageJ software are shown. (**A**) On this sagittal CT scan slice, a line connects the anterior and posterior acetabular margins to enclose the entire acetabulum. (**B**) After the acetabular margins are traced, the fill tool is used to define a volume mask over the area enclosed by the acetabulum.

on a 3-D CT reconstruction model. CT scans of the pelvis were obtained according to a standardized protocol. The 3-D CT reconstruction model was created after the two-dimensional (2-D) CT images were imported into an open-source software package (ImageJ v1.45i; NIH, Bethesda, MD, USA) [31] and further processed by an author not involved in the clinical care of the patients (JR). The margins of the acetabulum were manually traced on each axial slice and the fill tool was used to define a mask over the area enclosed by the acetabulum (Fig. 1). The acetabular area was calculated for each axial image by summing the pixels at the mask intensity using the built-in threshold function. The volume of the acetabulum was then defined by summing the acetabular area in each of the axial images. A polygonal surface representing the acetabulum was created from the CT voxel data using the 3-D visualization tools [19]. A resampling factor of two was used to smooth the surface mesh. The model was subsequently exported as a Drawing Interchange Format (DXF) file from ImageJ into the software Mimics® 15 (Materialise, Leuven, Belgium) for further analysis. The volume (cubic millimeters) enclosed by the acetabular surface was then calculated. The femur and acetabulum were further defined by performing a thresholding operation on each axial image. Manual editing tools were used to define the joint cavity and ensure the femur was not merged with the acetabulum. DXF files of the proximal femoral and acetabular surfaces were created and exported from ImageJ to Mimics®. Surface editing tools in Mimics® were used to remove any overlapping triangles or voids in the polygonal surface mesh. A Laplacian first-order smoothing operation was performed to reduce the presence of artificial asperities on the surface using a 0.7 smoothing factor and three iterations. The acetabular surface area was defined by performing a cutting operation along the acetabular ridge [43]. All elements of the model falling inside this region were used to measure the acetabular surface area (square centimeters). The total femoral surface area (square centimeters) was defined by cutting along the head-neck junction and removing all remaining surfaces from the model [43] (Fig. 2). The area of the femoral head covered by the acetabulum was defined by viewing the complete 3-D model normal to the coronal plane. The model was then revolved around the axis normal to the sagittal plane such that no rotation in the transverse and coronal planes was permitted. This method was chosen to ensure interpatient surface measurements were consistent. Any visible portions of the femur not covered by the acetabulum were resected from the 3-D model via a cutting operation (Fig. 3). The remaining surface was used to define the area of femoral head covered by the acetabulum (square centimeters). The percentage of the femoral head covered by the acetabulum was calculated as the ratio of femoral head surface area covered by the acetabulum to the total area of the femoral head × 100 as previously described [12].

Acetabular version, acetabular osseous support, femoral NSA, and femoral version were assessed on 2-D CT scans of the pelvis obtained according to a standardized protocol. Patients were scanned supine with the pelvis in a neutral position. Contiguous axial images through the hip were acquired helically on either a single-detector CT scanner at 1.00-mm thickness or on a multidetector CT scanner at 0.624-section thickness and reconstructed at 1.25 mm using a bone algorithm. Images were acquired from the iliac crest through the lesser trochanter of the femur. Axial images through the distal femur were included to measure femoral version. All images were evaluated on a Picture Archiving and Communication workstation (Synapse®; Fujifilm Corp, Tokyo, Japan). Measurements were made with an electronic caliper and/or angle tool by a single experienced radiologist (SDB). To determine the spatial orientation of the acetabulum, the acetabular version angle was measured from axial CT scan images as the angle between the line connecting the anterior and posterior margins of acetabulum and a line perpendicular to the center line (the line connecting the femoral heads). Acetabular version angle measurements

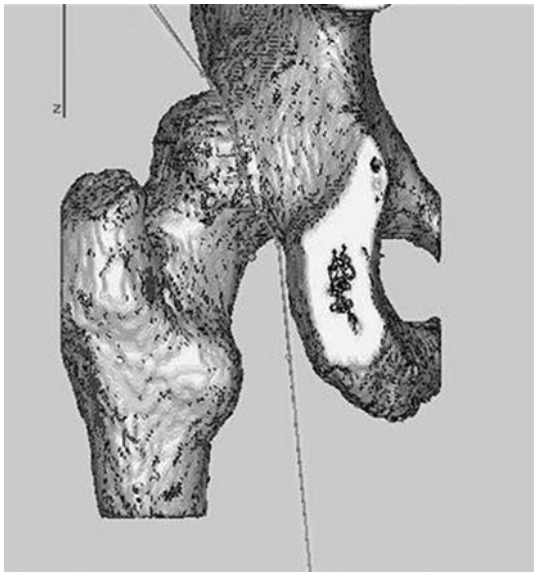

Fig. 2 The cutting procedure utilized in Mimics® to define the area of the femoral head covered by the acetabulum is shown.

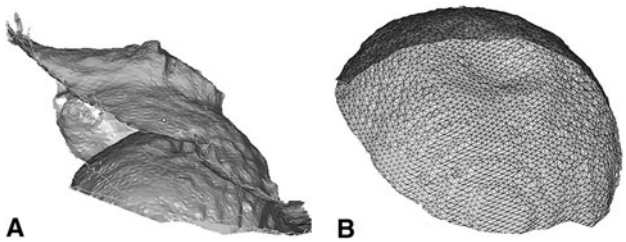

Fig. 3A–B (**A**) An example of a typical acetabular and femoral head surface area model is shown. (**B**) A polygonal mesh of the femoral head surface is shown.

were obtained at the following levels, relative to the acetabular roof: 5 mm (Level I), 10 mm (Level II), 15 mm (Level III), 20 mm (Level IV), and 25 mm (Level V, the closest to the center of the femoral head) [2] (Fig. 4). To determine the anterior and posterior acetabular bony support for the femoral head, the anterior acetabular sector angle and the posterior acetabular sector angle were measured on axial images at the level of the center of the acetabulum [2] (Fig. 4). The anterior acetabular sector angle was measured as the angle between the center line, the line connecting the femoral heads, and a line from the center of the femoral head to the anterior margin of acetabulum [2]. The posterior acetabular sector angle was defined by the angle between the center line and a line from the center of the femoral head to the posterior margin of acetabulum [2]. Severity of coxa valga was determined by measurement of the femoral NSA on a reformatted coronal-plane CT scan at the level of the center of the femoral head. Femoral NSA was measured on a reformatted coronal-plane CT scan at the level of the center of the femoral head. The femoral NSA was defined by the angle between a line through the axis of the femoral neck and a line through the longitudinal axis of the femoral shaft [6]. Femoral version was measured as the angle between a line bisecting the long axis of the femoral neck (from the center of the femoral head to center of the femoral neck) and a horizontal line [30]. Femoral version was corrected for rotation at the level of the femoral condyles by measuring the angle between the posterior intercondylar line and a horizontal line.

The osteoarthritis grade was assessed on AP pelvic radiographs using the grading scheme of Tönnis [37]. A normal joint space with no acetabular roof sclerosis was graded as 0, joint space narrowing with widened sclerotic zone and minimal osteophyte formation as 1, moderate loss of joint space with cystic formation as 2, and severe loss of joint space (< 1 mm) as 3.

Descriptive statistics were used to summarize the demographics and clinical characteristics of all patients included in the analysis. Chi-square, Fisher's exact, and Student's t-tests, when appropriate, were used to compare the distribution of demographics in the two groups. Linear regression analyses were used to compare measurements obtained from plain radiographs, 2-D CT scans, and the 3-D finite element analysis between the CMTHD and DDH groups. An alpha value of 0.05 or less was considered statistically significant. All statistical analyses were performed with SAS® Version 9.3 (SAS Institute Inc, Cary, NC, USA).

Results

Acetabular dysplasia was more severe in CMTHD than in DDH, as measured by plain AP and false-profile radiographs and 3-D CT reconstruction models (Table 2). Analysis of plain radiographs revealed the mean LCEA (mean difference, −11°; 95% CI: −18° to −5°; $p < 0.001$) and mean ACEA (mean difference, −21°; 95% CI: −29° to −12°; $p < 0.001$) were significantly lower while the mean TA was significantly higher (mean difference, 5.5°; 95% CI: 0.7°–10°; $p = 0.025$) in the CMTHD group than in the DDH group. CMTHD hips demonstrated a significantly lower acetabular volume (mean difference, −4.2 cm^3; 95% CI: −7.6 to −0.7 cm^3; $p = 0.018$) than DDH hips. Hip subluxation was also more severe in CMTHD (Table 2), as demonstrated by a lower area of the femoral head covered by the acetabulum (mean difference, −3.7 cm^2; 95% CI: −1.4 to 12 cm^2; $p = 0.034$) and lower percentage of the femoral head covered by the acetabulum (mean difference, −15%; 95% CI: −25% to −6.5%; $p = 0.007$).

CMTHD hips demonstrated higher degrees of acetabular anteversion and more deficient osseous support to the

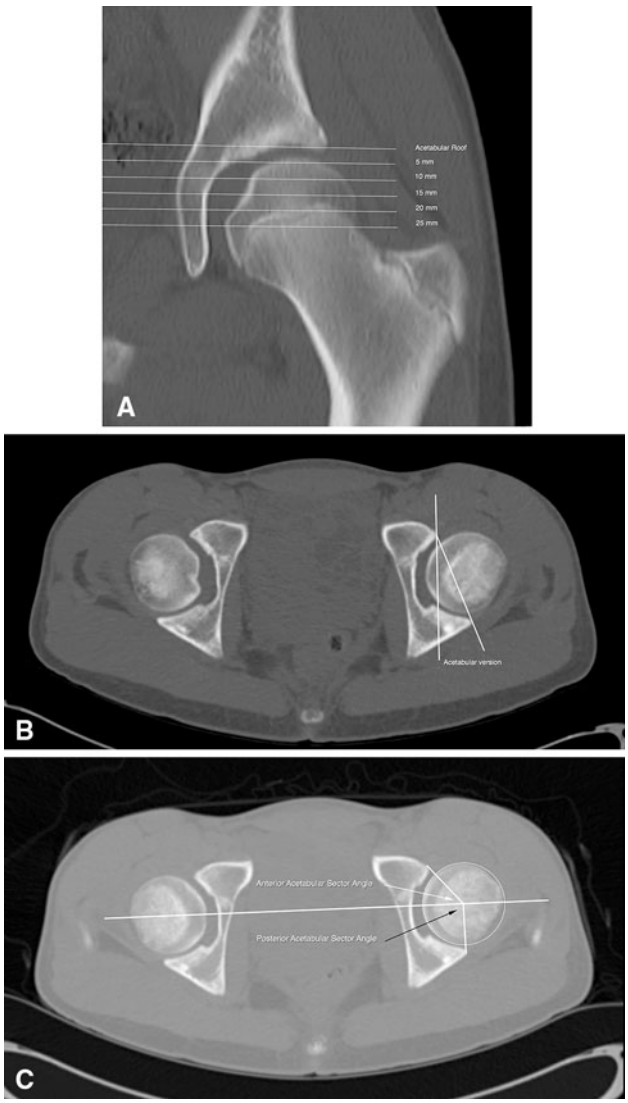

Fig. 4A–C Methods of measuring acetabular version and acetabular sector angles are shown. (**A**) In this coronal CT slice through the center of the femoral head, the acetabular version is measured in 5-mm increments beginning at the acetabular roof extending distally. (**B**) In this axial CT slice, acetabular version is the angle formed by the intersection of a line from the anterior to the posterior acetabular margins and a perpendicular line to the transverse axis of the pelvis. (**C**) The anterior acetabular sector angle (white arrow) is formed by the intersection of a line connecting the center of the femoral head to the anterior edge of the acetabulum and the transverse axis of the pelvis connecting the center of both femoral heads. The posterior acetabular sector angle (black arrow) is the angle formed by the intersection of a line connecting the center of the femoral head to the posterior edge of the acetabulum and the transverse axis of the pelvis connecting the center of the femoral heads.

femoral head (Table 3). The mean acetabular version angle was significantly higher in the CMTHD group than in the DDH group at all levels measured: Level I (mean difference, 12°, 95% CI: 8°–16°; $p < 0.001$), Level II (mean difference, 11°; 95% CI: 6°–16°; $p < 0.001$), Level III (mean difference, 10°; 95% CI, 4.9°–14°; $p < 0.001$), Level IV (mean difference, 7°; 95% CI: 2.9°–11°; $p = 0.001$), and Level V (mean difference, 4.2°; 95% CI: 0.1°–8°; $p = 0.043$). Anterior and posterior acetabular support were more deficient in the CMTHD group than in the DDH group, as evidenced by significantly lower anterior acetabular section angle (mean difference, −21°; 95% CI, −28° to −14°; $p < 0.001$) and posterior acetabular section angle (mean difference, −6.8; 95% CI, −12° to 1.9°; $p = 0.0072$).

Coxa valga was more severe in CMTHD than in DDH (Table 3), as measured by a significantly higher femoral NSA (mean difference, 8.7°; 95% CI, 3.7°–14°; $p < 0.001$). In contrast, there was no difference in femoral version ($p = 0.104$) between groups.

Osteoarthritis of the hip was significantly ($p = 0.006$) more prevalent in the CMTHD group (Table 2). No patient in the DDH group presented with hip osteoarthritis while three of 19 hips in the CMTHD group presented with moderate arthritis (Tönnis Grade 2) and one with severe arthritis (Tönnis Grade 3).

Discussion

The complex 3-D geometry of the acetabulum and the pattern of acetabular insufficiency should be recognized to apply the appropriate corrective osteotomy of the pelvis and/or femur associated with hip dysplasia. Nevertheless, the pathoanatomy of the dysplastic hip in CMT is not well described in the literature. Therefore, in this study, we performed a morphometric comparison of the acetabulum and proximal femur in 19 hips affected by CMTHD and 45 hips affected by DDH. We found that patients with CMTHD in general had more severe acetabular dysplasia, greater acetabular anteversion with less anterior and posterior acetabular osseous support to the femoral head, more severe coxa valga, and higher prevalence of arthritis at the time of presentation for PAO than patients with DDH.

We acknowledge several limitations of this study. First, our search criteria included only patients who had undergone PAO, which could lead to a selection bias because some pediatric patients with other types of hip surgery were not included. Although the sample size was relatively small, to our knowledge, this is the first series of CMTHD analyzed by standard radiographic and CT scans methods. Second, a single observer performed measurements on radiographs (ENN), axial CT scans (SDB), and 3-D CT reconstruction models (JR). Interobserver and intraobserver reliability for plain radiographs parameters in adults with hip dysplasia have been reported to be moderate to excellent [26, 35]. Intraobserver and interobserver reliability for the acetabular version, anterior acetabular sector angle, and posterior acetabular sector angle have also been reported to

Table 2. Comparison of severity of acetabular dysplasia, hip subluxation, and osteoarthritis based on plain radiographs and 3-D CT reconstruction models

Variable	CMTHD group (n = 19 hips)	DDH group (n = 45 hips)	p value
Lateral center-edge angle (°)*,†	−14 (−50 to 11)	−2 (−24 to 21)	0.001
Anterior center-edge angle (°)*,†	−13 (−40 to 16)	8 (−27 to 33)	< 0.001
Tönnis angle (°)*,†	31 (16–51)	25 (10–49)	0.025
Acetabular volume (cm^3)*,‡	27(18–35)	31 (20–46)	0.018
Total femoral head area (cm^2)*,‡	51 (28–78)	46 (24–72)	0.121
Total acetabular area (cm^2)*,‡	39 (19–58)	35 (21–58)	0.103
Area of femoral head covered by acetabulum (cm^2)*,‡	22 (12–31)	26 (16–38)	0.034
Percentage of femoral head covered by the acetabulum (%)*,‡	45 (25–68)	54 (35–79)	0.007
Tönnis grade (number of hips)			0.006
Arthritic (Grade 2 or 3)	4 (22%)	0 (0%)	
Nonarthritic (Grade 0 or 1)	14 (78%)	42 (100%)	

* Values are expressed as mean, with range in parentheses; †measurement based on plain radiographs; ‡measurement based on 3-D CT reconstruction models; 3-D = three-dimensional; CMTHD = Charcot-Marie-Tooth hip dysplasia; DDH = developmental dysplasia of the hip.

Table 3. Comparison of acetabular version, acetabular osseous support to the femoral head, coxa valga, and femoral version based on 2-D CT scans

Variable	CMTHD group (n = 19 hips)	DDH group (n = 45 hips)	p value
Acetabular version (°)*			
Level I	14 (−60 to 27)	2 (−13 to 15)	< 0.001
Level II	18 (−7 to 32)	7 (−15 to 24)	< 0.001
Level III	22 (−7 to 31)	12 (−7 to 31)	< 0.001
Level IV	24 (−1 to 35)	16 (−8 to 31)	0.001
Level V	24 (3–35)	19 (−2 to 32)	0.043
Anterior acetabular sector angle (°)*	30 (10–56)	51 (22–92)	< 0.001
Posterior acetabular sector angle (°)*	80 (56–102)	87 (72–100)	0.007
Coxa valga (femoral neck-shaft angle) (°)†	156 (141–175)	148 (130–168)	< 0.001
Femoral version (°)*	28 (7–47)	22 (−21 to 46)	0.104

Values are expressed as mean, with range in parentheses; * measurement based on axial 2-D CT scans; †measurement based on coronal 2-D CT scans; 2-D = two-dimensional; CMTHD = Charcot-Marie-Tooth hip dysplasia; DDH = developmental dysplasia of the hip.

be excellent [11], with intraobserver reproducibility (95% limits of agreement) for acetabular version within 3.43° (range, −2.02° to 3.43°) [13]. Intraobserver variability in measurements of the percentage of the femoral head covered by the acetabulum was reported to range from 0% to 7.8%, with overall average intraobserver differences of only 1.4% [12]. Third, because of the limited sample size of the CMT group, we were not able to evaluate the relation between potential differences specific to age and sex. Fourth, although our data showed a more severe pattern of dysplasia in the CMTHD cohort than in the DDH cohort, the clinical consequences and impact on surgical reconstruction are yet to be determined.

We found a more severe degree of acetabular dysplasia and hip subluxation in CMTHD than in DDH. The severity of CMTHD assessed by the LCEA, ACEA, and TA are in agreement with measurements described in previous studies on pelvic osteotomies for the treatment of severe hip dysplasia with marked subluxation or the presence of a false acetabulum [8, 28]. Previous studies evaluating short- and medium-term results of PAO for the treatment of hip dysplasia reported comparable radiographic measurements found in the DDH group [9, 21, 32, 33]. We also found lower acetabular volume in CMTHD than in DDH. The difference in acetabular dysplasia between CMTHD and DDH may be related to the neuromuscular progressive nature of CMT. Weakness of the proximal musculature of the hip gradually increases over time, aggravating the degree of acetabular dysplasia and hip subluxation [7, 16, 17, 27]. It is well recognized that patients with CMTHD do not develop symptoms until early adulthood, which may correspond to advanced subluxation of the hip [16, 40, 42]. We found more severe subluxation of the hip in CMTHD compared to DDH as measured on 3-D CT reconstruction models. Previous studies have used 3-D CT models to assess the severity of hip subluxation by measuring the percentage of the femoral head covered by the acetabulum. Normal values have been reported to range from 73% to 89% [10, 12] compared to 51% to 65% in DDH [10, 12, 25]. Compared to the literature, our data showed a higher degree of subluxation in CMTHD hips, with an average of 45% of femoral head area covered by the acetabulum. The area of the femoral head area covered by the acetabulum has been reported to measure around 26 cm^2 in normal individuals [43]. This value is higher than the value we reported for CMTHD but is comparable to that of our DDH cohort.

We reported a higher degree of acetabular anteversion in the CMTHD group compared to the DDH group. While normal values ranging from 15° to 20° have been reported [2, 12, 30, 34], dysplastic hips have typically been

associated with higher anteversion ranging from 21° to 23° [3, 12]. In both groups, the acetabular version increased as the level of measurement moved from cranial to caudal. This phenomenon has been previously described for DDH [3, 11] but not for normal hips [2]. In CMTHD hips, however, acetabular anteversion was consistently more severe than in DDH hips at every level measured. Understanding acetabular version is important before surgical correction of hip dysplasia, as both excessive acetabular anteversion and acetabular retroversion have been described as negative predictive factors for survivorship after PAO [1].

Measurements of the acetabular sector angles demonstrated that the acetabular osseous support was severely reduced in the CMTHD hips. Acetabular sector angles were described in the past as a measure of acetabular support to the femoral head. Anda et al. [2, 4] distinguished acetabular coverage (part of the acetabulum primarily concerned with weightbearing in the standing position) from acetabular support (nonweightbearing portions of the acetabulum that contribute to containing the femoral head). Normal values for the anterior acetabular sector angle were determined to be 64° ± 6.1° for males and 63° ± 6.1° for females, while those for posterior sector angles were 102° ± 8.4° for males and 105° ± 7.9° for females [2]. In hip dysplasia, both the anterior and posterior acetabular sector angles are lower when compared to normal reference values [2–4, 12, 23]. In this study, measurements of anterior and posterior acetabular sector angles for the DDH cohort were in line with previous studies [3, 4, 12, 23]. In the CMTHD hips, however, the mean acetabular support angles were significantly lower anteriorly and posteriorly when compared to the DDH hips, indicating a severe globally insufficient acetabular osseous support to the femoral head [12]. This information is important when correcting dysplastic hips secondary to CMT because 3-D reorientation of the acetabulum is necessary and this may only be achieved with a complete PAO.

Using coronal reformatted CT scans, femoral NSA was on average higher in patients with CMTHD than in patients with DDH; however, we did not find a significant difference in femoral version between the groups. Although coxa valga and excessive femoral anteversion have been described as part of the abnormal hip morphology in CMTHD [7, 16, 29, 42], we are unaware of studies investigating femoral version in CMT. In our study, femoral version in CMTHD and DDH measured higher than previous measurements reported as normal ranging from 15° to 20° [38]. Walker et al. [42] reviewed pelvic radiographs of 74 children with CMT and reported a high prevalence of coxa valga. The authors however could not draw any conclusion about femoral torsion. Although it would be intuitive to consider a correction of the valgus-anteversion deformity by means of an intertrochanteric femoral osteotomy, this technique is controversial in patients with CMT because of the risk of further weakening the hip abductors [7, 16]. Excessive femoral anteversion associated with the excessive acetabular anteversion and insufficient anterior osseous support contributes to the severe pattern of subluxation of the hip reported in the CMTHD group.

In our study, there was a higher prevalence of moderate and severe osteoarthritis in patients with CMTHD than in patients with DDH at time of presentation for PAO. We are unaware of previous studies investigating the prevalence of osteoarthritis in CMTHD. However, previous studies have postulated that patients with CMT do not develop symptoms until later when subluxation and signs of arthritis may be present [29]. Our findings confirm this hypothesis.

In this study, the degree of acetabular dysplasia and hip subluxation were greater in a cohort of patients affected by CMTHD relative to a matched group of patients with DDH. Patients with CMTHD tended to have a global acetabular insufficiency with more severe dysplasia and less femoral head coverage, higher acetabular anteversion, less anterior and posterior acetabular osseous support, and more severe coxa valga than patients with hip dysplasia secondary to DDH. In addition, we observed a higher prevalence of moderate and severe osteoarthritis in the CMTHD cohort. Previous studies have recommended screening patients with CMT for hip dysplasia during childhood [7, 16]. Earlier diagnosis would allow early intervention, potentially avoiding the silent progression of hip dysplasia into the severe pattern described in this series. Further studies would be necessary to investigate whether screening and early intervention are warranted. Understanding the dysplasia severity, acetabular orientation, and pattern of femoral head insufficient coverage is crucial in planning for the appropriate acetabular or femoral corrective osteotomy. We have implemented a routine use of preoperative CT scans for planning the desired correction in patients with CMTHD who are candidates for a pelvic osteotomy. We currently believe the Bernese PAO allows for reorientation of the dysplastic acetabulum in CMTHD. Nevertheless, future clinical research is needed to investigate the clinical and functional outcomes of patients with CMT undergoing pelvic or femoral osteotomies and to define the role of surgical intervention in this complex type of hip dysplasia.

Acknowledgments We acknowledge the help of Kerri Murray and Gloria Boyen in gathering the data for this study.

References

1. Albers CE, Steppacher SD, Ganz R, Tannast M, Siebenrock KA. Impingement adversely affects 10-year survivorship after

periacetabular osteotomy for DDH. *Clin Orthop Relat Res.* 2013;471:1602–1614.
2. Anda S, Svenningsen S, Dale LG, Benum P. The acetabular sector angle of the adult hip determined by computed tomography. *Acta Radiol Diagn (Stockh).* 1986;27:443–447.
3. Anda S, Terjesen T, Kvistad KA. Computed tomography measurements of the acetabulum in adult dysplastic hips: which level is appropriate? *Skeletal Radiol.* 1991;20:267–271.
4. Anda S, Terjesen T, Kvistad KA, Svenningsen S. Acetabular angles and femoral anteversion in dysplastic hips in adults: CT investigation. *J Comput Assist Tomogr.* 1991;15:115–120.
5. Bamford NS, White KK, Robinett SA, Otto RK, Gospe SM Jr. Neuromuscular hip dysplasia in Charcot-Marie-Tooth disease type 1A. *Dev Med Child Neurol.* 2009;51:408–411.
6. Buller LT, Rosneck J, Monaco FM, Butler R, Smith T, Barsoum WK. Relationship between proximal femoral and acetabular alignment in normal hip joints using 3-dimensional computed tomography. *Am J Sports Med.* 2012;40:367–375.
7. Chan G, Bowen JR, Kumar SJ. Evaluation and treatment of hip dysplasia in Charcot-Marie-Tooth disease. *Orthop Clin North Am.* 2006;37:203–209, vii.
8. Clohisy JC, Barrett SE, Gordon JE, Delgado ED, Schoenecker PL. Periacetabular osteotomy for the treatment of severe acetabular dysplasia. *J Bone Joint Surg Am.* 2005;87:254–259.
9. Clohisy JC, Schutz AL, St John L, Schoenecker PL, Wright RW. Periacetabular osteotomy: a systematic literature review. *Clin Orthop Relat Res.* 2009;467:2041–2052.
10. Dandachli W, Kannan V, Richards R, Shah Z, Hall-Craggs M, Witt J. Analysis of cover of the femoral head in normal and dysplastic hips: new CT-based technique. *J Bone Joint Surg Br.* 2008;90:1428–1434.
11. Fujii M, Nakashima Y, Yamamoto T, Mawatari T, Motomura G, Matsushita A, Matsuda S, Jingushi S, Iwamoto Y. Acetabular retroversion in developmental dysplasia of the hip. *J Bone Joint Surg Am.* 2010;92:895–903.
12. Ito H, Matsuno T, Hirayama T, Tanino H, Yamanaka Y, Minami A. Three-dimensional computed tomography analysis of non-osteoarthritic adult acetabular dysplasia. *Skeletal Radiol.* 2009; 38:131–139.
13. Kim WY, Hutchinson CE, Andrew JG, Allen PD. The relationship between acetabular retroversion and osteoarthritis of the hip. *J Bone Joint Surg Br.* 2006;88:727–729.
14. Kohnlein W, Ganz R, Impellizzeri FM, Leunig M. Acetabular morphology: implications for joint-preserving surgery. *Clin Orthop Relat Res.* 2009;467:682–691.
15. Krajewski KM, Lewis RA, Fuerst DR, Turansky C, Hinderer SR, Garbern J, Kamholz J, Shy ME. Neurological dysfunction and axonal degeneration in Charcot-Marie-Tooth disease type 1A. *Brain.* 2000;123(pt 7):1516–1527.
16. Kumar SJ, Marks HG, Bowen JR, MacEwen GD. Hip dysplasia associated with Charcot-Marie-Tooth disease in the older child and adolescent. *J Pediatr Orthop.* 1985;5:511–514.
17. Kuruvilla A, Costa JL, Wright RB, Yoder DM, Andriacchi TP. Characterization of gait parameters in patients with Charcot-Marie-Tooth disease. *Neurol India.* 2000;48:49–55.
18. Lequesne M, de Sèze S. [False profile of the pelvis: a new radiographic incidence for the study of the hip: its use in dysplasias and different coxopathies] [in French]. *Rev Rhum Mal Osteoartic.* 1961;28:643–652.
19. Lorensen WE, Cline HE. Marching cubes: a high resolution 3D surface construction algorithm. *ACM SIGGRAPH Computer Graphics.* 1987;21:163–169. 45
20. Mandel DM, Loder RT, Hensinger RN. The predictive value of computed tomography in the treatment of developmental dysplasia of the hip. *J Pediatr Orthop.* 1998;18:794–798.
21. Matheney T, Kim YJ, Zurakowski D, Matero C, Millis M. Intermediate to long-term results following the Bernese periacetabular osteotomy and predictors of clinical outcome. *J Bone Joint Surg Am.* 2009;91:2113–2123.
22. McGann R, Gurd A. The association between Charcot-Marie-Tooth disease and developmental dysplasia of the hip. *Orthopedics.* 2002;25:337–339.
23. Murphy SB, Kijewski PK, Millis MB, Harless A. Acetabular dysplasia in the adolescent and young adult. *Clin Orthop Relat Res.* 1990;261:214–223.
24. Nakahara I, Takao M, Sakai T, Nishii T, Yoshikawa H, Sugano N. Gender differences in 3D morphology and bony impingement of human hips. *J Orthop Res.* 2011;29:333–339.
25. Nakamura S, Yorikawa J, Otsuka K, Takeshita K, Harasawa A, Matsushita T. Evaluation of acetabular dysplasia using a top view of the hip on three-dimensional CT. *J Orthop Sci.* 2000;5:533–539.
26. Nelitz M, Guenther KP, Gunkel S, Puhl W. Reliability of radiological measurements in the assessment of hip dysplasia in adults. *Br J Radiol.* 1999;72:331–334.
27. Newman CJ, Walsh M, O'Sullivan R, Jenkinson A, Bennett D, Lynch B, O'Brien T. The characteristics of gait in Charcot-Marie-Tooth disease types I and II. *Gait Posture.* 2007;26:120–127.
28. Ninomiya S. Rotational acetabular osteotomy for the severely dysplastic hip in the adolescent and adult. *Clin Orthop Relat Res.* 1989;247:127–137.
29. Pailthorpe CA, Benson MK. Hip dysplasia in hereditary motor and sensory neuropathies. *J Bone Joint Surgery Br.* 1992;74:538–540.
30. Perreira AC, Hunter JC, Laird T, Jamali AA. Multilevel measurement of acetabular version using 3-D CT-generated models: implications for hip preservation surgery. *Clin Orthop Relat Res.* 2011;469:552–561.
31. Schneider CA, Rasband WS, Eliceiri KW. NIH Image to ImageJ: 25 years of image analysis. *Nat Methods.* 2012;9:671–675.
32. Siebenrock KA, Leunig M, Ganz R. Periacetabular osteotomy: the Bernese experience. *Instr Course Lect.* 2001;50:239–245.
33. Steppacher SD, Tannast M, Ganz R, Siebenrock KA. Mean 20-year followup of Bernese periacetabular osteotomy. *Clin Orthop Relat Res.* 2008;466:1633–1644.
34. Tallroth K, Lepisto J. Computed tomography measurement of acetabular dimensions: normal values for correction of dysplasia. *Acta Orthop.* 2006;77:598–602.
35. Terjesen T, Gunderson RB. Reliability of radiographic parameters in adults with hip dysplasia. *Skeletal Radiol.* 2012;41:811–816.
36. Thawrani D, Sucato DJ, Podeszwa DA, DeLaRocha A. Complications associated with the Bernese periacetabular osteotomy for hip dysplasia in adolescents. *J Bone Joint Surg Am.* 2010;92: 1707–1714.
37. Tönnis D. General radiograph of the hip joint. In: Tönnis D, ed. *Congenital Dysplasia, Dislocation of the Hip.* New York, NY: Springer; 1987:100–142.
38. Tönnis D, Heinecke A. Acetabular and femoral anteversion: relationship with osteoarthritis of the hip. *J Bone Joint Surg Am.* 1999;81:1747–1770.
39. Trumble SJ, Mayo KA, Mast JW. The periacetabular osteotomy: minimum 2 year followup in more than 100 hips. *Clin Orthop Relat Res.* 1999;363:54–63.
40. Ushiyama T, Tanaka C, Kawasaski T, Matsusue Y. Hip dysplasia in Charcot-Marie-Tooth disease: report of a family. *J Orthop Sci.* 2003;8:610–612.
41. van Erve RH, Driessen AP. Developmental hip dysplasia in hereditary motor and sensory neuropathy type 1. *J Pediatr Orthop.* 1999;19:92–96.
42. Walker JL, Nelson KR, Heavilon JA, Stevens DB, Lubicky JP, Ogden JA, VandenBrink KA. Hip abnormalities in children with Charcot-Marie-Tooth disease. *J Pediatr Orthop.* 1994;14:54–59.

43. Weaver AA, Gilmartin TD, Anz AW, Stubbs AJ, Stitzel JD. A method to measure acetabular metrics from three dimensional computed tomography pelvis reconstructions—biomed 2009. *Biomed Sci Instrum.* 2009;45:155–160.
44. Weiner LS, Kelley MA, Ulin RI, Wallach D. Development of the acetabulum and hip: computed tomography analysis of the axial plane. *J Pediatr Orthop.* 1993;13:421–425.
45. Wiberg G. Studies on dysplastic acetabula and congenital subluxation of the hip joint: with special reference to the complication of osteo-arthritis. *Acta Chir Scand.* 1939;83(suppl 58):5–135.
46. Yagerman SE, Cross MB, Green DW, Scher DM. Pediatric orthopedic conditions in Charcot-Marie-Tooth disease: a literature review. *Curr Opin Pediatr.* 2012;24:50–56.